

CHAPTER 63

CRYOGENIC SYSTEMS

Leonard A. Wenzel
Lehigh University
Bethlehem, Pennsylvania

63.1 CRYOGENICS AND CRYOFLUID PROPERTIES	1915	63.5.1 Materials of Construction	1943
		63.5.2 Seals and Gaskets	1953
		63.5.3 Lubricants	1953
63.2 CRYOGENIC REFRIGERATION AND LIQUEFACTION CYCLES	1921	63.6 SPECIAL PROBLEMS IN LOW-TEMPERATURE INSTRUMENTATION	1953
63.2.1 Cascade Refrigeration	1921	63.6.1 Temperature Measurement	1953
63.2.2 The Linde or Joule-Thomson Cycle	1923	63.6.2 Flow Measurement	1955
63.2.3 The Claude or Expander Cycle	1924	63.6.3 Tank Inventory Measurement	1955
63.2.4 Low-Temperature Engine Cycles	1928	63.7 EXAMPLES OF CRYOGENIC PROCESSING	1955
63.3 CRYOGENIC HEAT-TRANSFER METHODS	1930	63.7.1 Air Separation	1956
63.3.1 Coiled-Tube-in-Shell Exchangers	1931	63.7.2 Liquefaction of Natural Gas	1958
63.3.2 Plate-Fin Heat Exchangers	1933	63.7.3 Helium Recovery and Liquefaction	1962
63.3.3 Regenerators	1933	63.8 SUPERCONDUCTIVITY AND ITS APPLICATIONS	1963
63.4 INSULATION SYSTEMS	1939	63.8.1 Superconductivity	1963
63.4.1 Vacuum Insulation	1940	63.8.2 Applications of Superconductivity	1966
63.4.2 Superinsulation	1941	63.9 CRYOBIOLOGY AND CRYOSURGERY	1969
63.4.3 Insulating Powders and Fibers	1943		
63.5 MATERIALS FOR CRYOGENIC SERVICE	1943		

63.1 CRYOGENICS AND CRYOFLUID PROPERTIES

The science and technology of deep refrigeration processing occurring at temperatures lower than about 150 K is the field of cryogenics (from the Greek *kryos*, icy cold). This area has developed as a special discipline because it is characterized by special techniques, requirements imposed by physical limitations, and economic needs, and unique phenomena associated with low-thermal-energy levels.

Compounds that are processed within the cryogenic temperature region are sometimes called cryogens. There are only a few of these materials; they are generally small, relatively simple molecules, and they seldom react chemically within the cryogenic region. Table 63.1 lists the major cryogens along with their major properties, and with a reference giving more complete thermodynamic data.

Table 63.1 Properties of Principal Cryogenes

Name	Normal Boiling Point			Critical Point		Triple Point		Reference
	T (K)	Liquid Density (kg/m ³)	Latent Heat (J/kg · mole)	T (K)	P (kPa)	T (K)	P (kPa)	
Helium	4.22	123.9	91,860	5.28	227			1
Hydrogen	20.39	70.40	902,300	33.28	1296	14.00	7.20	2, 3
Deuterium	23.56	170.0	1,253,000	38.28	1648	18.72	17.10	4
Neon	27.22	1188.7	1,737,000	44.44	2723	26.28	43.23	5
Nitrogen	77.33	800.9	5,579,000	126.17	3385	63.22	12.55	6
Air	78.78	867.7	5,929,000					7, 8
Carbon monoxide	82.11	783.5	6,024,000	132.9	3502	68.11	15.38	9
Fluorine	85.06	1490.6	6,530,000	144.2	5571			10
Argon	87.28	1390.5	6,504,000	151.2	4861	83.78		11, 12, 13
Oxygen	90.22	1131.5	6,801,000	154.8	5081	54.39	0.14	6
Methane	111.72	421.1	8,163,000	190.61	4619	90.67	11.65	14
Krypton	119.83	2145.4	9,009,000	209.4	5488	116.00	73.22	15
Nitric oxide	121.50	1260.2	13,809,000	179.2	6516	108.94		
Nitrogen trifluoride	144.72	1525.6	11,561,000	233.9	4530			
Refrigerant-14	145.11	1945.1	11,969,000	227.7	3737	89.17	0.12	16
Ozone	161.28	1617.8	14,321,000	261.1	5454			
Xenon	164.83	3035.3	12,609,000	289.8	5840	161.39	81.50	17
Ethylene	169.39	559.4	13,514,000	282.7	5068	104.00	0.12	18

All of the cryogenics except hydrogen and helium have conventional thermodynamic and transport properties. If specific data are unavailable, the reduced properties correlation can be used with all the cryogenics and their mixtures with at least as much confidence as the correlations generally allow. Qualitatively T - S and P - H diagrams such as those of Figs. 63.1 and 63.2 differ among cryogenics only by the location of the critical point and freezing point relative to ambient conditions.

Air, ammonia synthesis gas, and some inert atmospheres are considered as single materials although they are actually gas mixtures. The composition of air is shown in Table 63.12. If a thermodynamic diagram for air has the lines drawn between liquid and vapor boundaries where the pressures are equal for the two phases, these lines will not be at constant temperature, as would be the case for a pure component. Moreover, these liquid and vapor states are not at equilibrium, for the equilibrium states have equal T s and P s, but differ in composition. That being so, one or both of these equilibrium mixtures is not air. Except for this difference the properties of air are also conventional.

Hydrogen and helium differ in that their molecular mass is small in relation to zero-point-energy levels. Thus quantum differences are large enough to produce measurable changes in gross thermodynamic properties.

Hydrogen and its isotopes behave abnormally because the small molecular weight allows quantum differences stemming from different molecular configurations to affect total thermodynamic properties. The hydrogen molecule consists of two atoms, each containing a single proton and a single electron. The electrons rotate in opposite directions as required by molecular theory. The protons, however, may rotate in opposed or parallel directions. Figure 63.3 shows a sketch of the two possi-

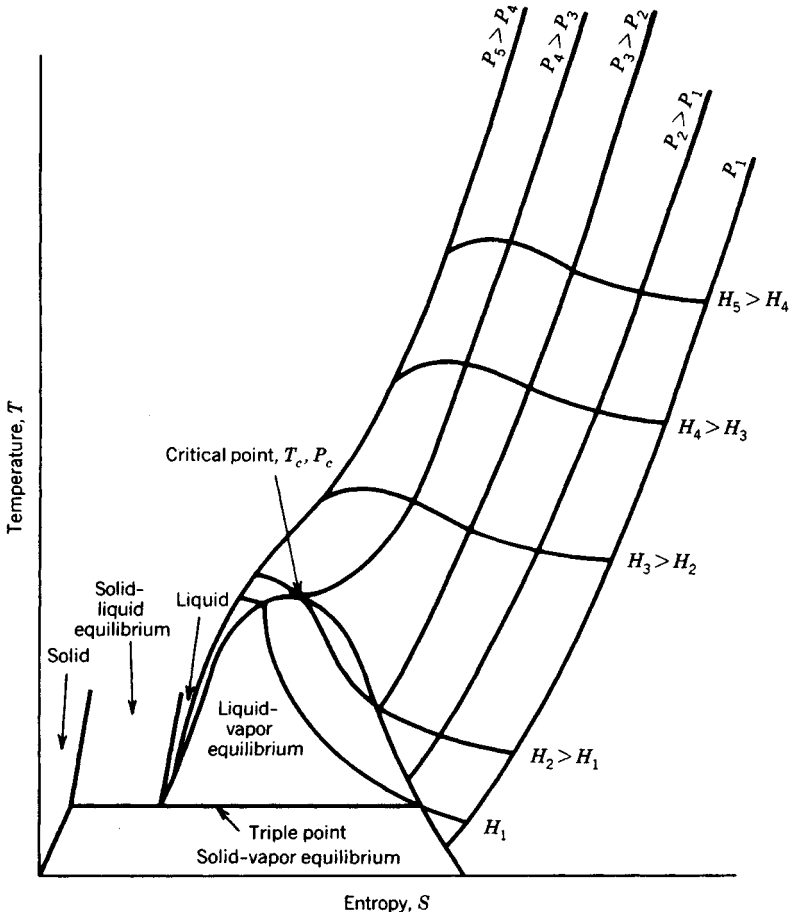


Fig. 63.1 Skeletal T - S diagram.

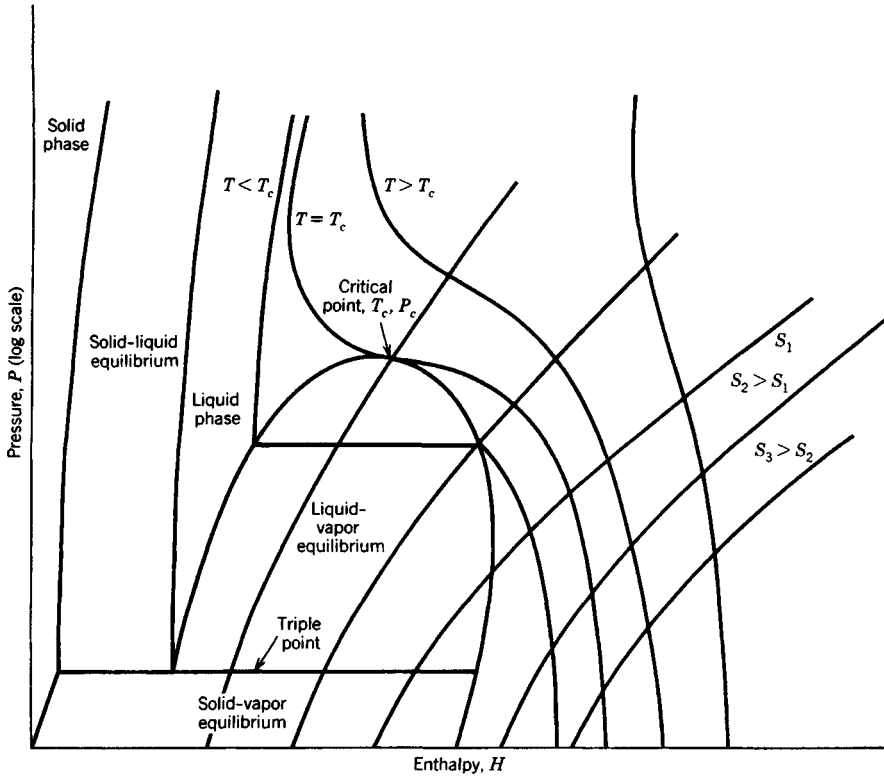


Fig. 63.2 Skeletal P - H diagram.

bilities, the parallel rotating nuclei identifying ortho-hydrogen and the opposite rotating nuclei identifying the parahydrogen. The quantum mechanics exhibited by these two molecule forms are different, and produce different thermodynamic properties. Ortho- and para-hydrogen each have conventional thermodynamic properties. However, ortho- and para-hydrogen are interconvertible with the equilibrium fraction of pure H_2 existing in para form dependent on temperature, as shown in Table 63.2. The natural ortho- and para-hydrogen reaction is a relatively slow one and of second order:¹⁹

$$\frac{dx}{d\theta} = 0.0114x^2 \quad \text{at } 20 \text{ K}$$

where θ is time in hours and x is the mole fraction of ortho-hydrogen. The reaction rate can be greatly accelerated by a catalyst that interrupts the molecular magnetic field and possesses high surface area. Catalysts such as NiO_2/SiO_2 have been able to yield some of the highest heterogeneous reaction rates measured.²⁰

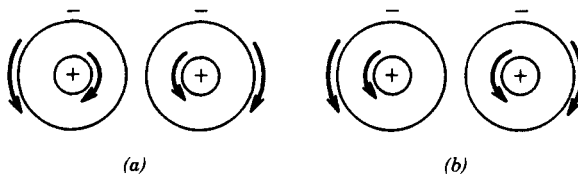


Fig. 63.3 Molecular configurations of (a) para- and (b) ortho-hydrogen.

Table 63.2 Equilibrium Para-Hydrogen Concentration as a Function of T (K)

T (K)	Equilibrium Percentage of Para-Hydrogen
20	99.82
30	96.98
40	88.61
60	65.39
80	48.39
100	38.51
150	28.54
273	25.13
500	25.00

Normally hydrogen exists as a 25 mole % p-H₂, 75 mole % o-H₂ mix. Upon liquefaction the hydrogen liquid changes to nearly 100% p-H₂. If this is done as the liquid stands in an insulated flask, the heat of conversion will suffice to evaporate the liquid, even if the insulation is perfect. For this reason the hydrogen is usually converted to para form during refrigeration by the catalyzed reaction, with the energy released added to the refrigeration load.

Conversely, liquid para-hydrogen has an enhanced refrigeration capacity if it is converted to the equilibrium state as it is vaporized and warmed to atmospheric condition. In certain applications recovery of this refrigeration is economically justifiable.

Helium, though twice the molecular weight of hydrogen, also shows the effects of flow molecular weight upon gross properties. The helium molecule is single-atomed and thus free from ortho-para-type complexities. Helium was liquefied conventionally first in 1908 by Onnes of Leiden, and the liquid phase showed conventional behavior at atmospheric pressure.

As temperature is lowered, however, a second-order phase change occurs at 2.18 K (0.05 atm) to produce a liquid called HeII. At no point does solidification occur just by evacuating the liquid. This results from the fact that the relationship between molecular volume, thermal energy (especially zero-point energy), and van der Waals attractive forces is such that the atoms cannot be trapped into a close-knit array by temperature reduction alone. Eventually, it was found that helium could be solidified if an adequate pressure is applied, but that the normal liquid helium (HeI)-HeII phase transition occurs at all pressures up to that of solidification. The phase diagram for helium is shown in Fig. 63.4. The HeI-HeII phase change has been called the lambda curve from the shape of the heat capacity curve for saturated liquid He, as shown in Fig. 63.5. The peculiar shape of the heat capacity curve produces a break in the curve for enthalpy of saturated liquid He as shown in Fig. 63.6.

HeII is a unique liquid exhibiting properties that were not well explained until after 1945. As liquid helium is evacuated to increasingly lower pressures, the temperature also drops along the vapor-pressure curve. If this is done in a glass vacuum-insulated flask, heat leaks into the liquid He causing boiling and bubble formation. As the temperature approaches 2.18 K, boiling gets more violent, but then suddenly stops. The liquid He is completely quiescent. This has been found to occur because the thermal conductivity of HeII is extremely large. Thus the temperature is basically constant and all boiling occurs from the surface where the hydrostatic head is least, producing the lowest boiling point.

Not only does HeII have very large thermal conductivity, but it also has near zero viscosity. This can be seen by holding liquid He in a glass vessel with a fine porous bottom such that normal He does not flow through. If the temperature is lowered into the HeII region, the helium will flow rapidly through the porous bottom. Flow does not seem to be enhanced or hindered by the size of the frit. Conversely, a propeller operated in liquid HeII will produce a secondary movement in a parallel propeller separated from the first by a layer of liquid HeII. Thus HeII has properties of finite and of infinitesimal viscosity.

These peculiar flow properties are also shown by the so-called thermal-gravimetric effect. There are two common demonstrations. If a tube with a finely fritted bottom is put into liquid HeII and the helium in the tube is heated, liquid flows from the main vessel into the fritted tube until the liquid level in the tube is much higher than that in the main vessel. A second, related, experiment uses a U-tube, larger on one leg than on the other with the two sections separated by a fine frit. If this tube is immersed, except for the end of the narrow leg, into liquid HeII and a strong light is

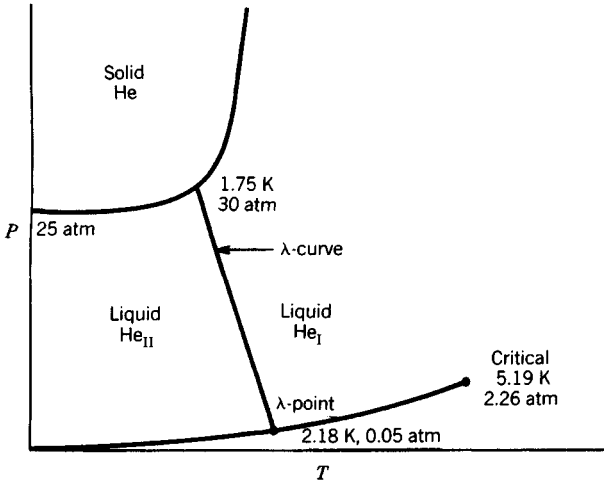


Fig. 63.4 Phase diagram for helium.

focused on the liquid He above the frit, liquid He will flow through the frit and out the small tube opening producing a fountain of liquid He several feet high.

These and other experiments²¹ can be explained through the quantum mechanics of HeII. The pertinent relationships, the Bose-Einstein equations, indicate that HeII has a dual nature: it is both a "superfluid" which has zero viscosity and infinite thermal conductivity among other special properties, and a fluid of normal properties. The further the temperature drops below the lambda point the greater the apparent fraction of superfluid in the liquid phase. However, very little superfluid is required. In the flow through the porous frit the superfluid flows, the normal fluid is retained. However, if the temperature does not rise, some of the apparently normal fluid will apparently become superfluid. Although the superfluid flows through the frit, there is no depletion of superfluid in the liquid He left behind. In the thermogravimetric experiments the superfluid flows through the frit but is then changed to normal He. Thus there is no tendency for reverse flow.

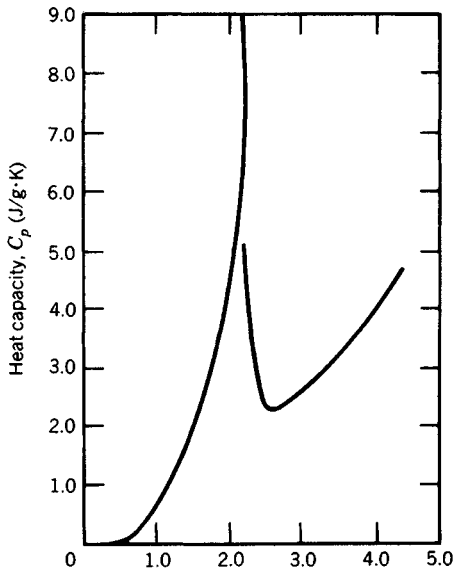


Fig. 63.5 Heat capacity of saturated liquid ⁴He.

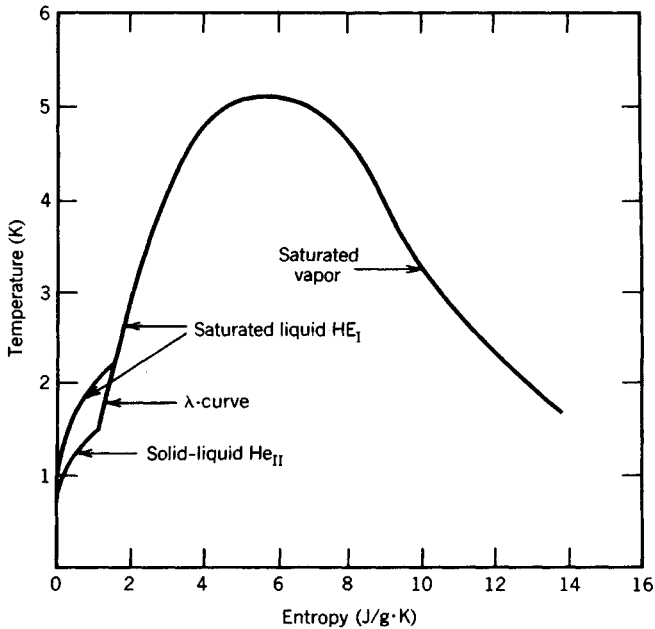


Fig. 63.6 Temperature-entropy diagram for saturation region of ^4He .

At this point applications have not developed for HeII . Still, the peculiar phase relationships and energy effects may influence the design of helium processes, and do affect the shape of thermodynamic diagrams for helium.

63.2 CRYOGENIC REFRIGERATION AND LIQUEFACTION CYCLES

One characteristic aspect of cryogenic processing has been its early and continued emphasis on process efficiency, that is, on energy conservation. This has been forced on the field by the very high cost of deep refrigeration. For any process the minimum work required to produce the process goal is

$$W_{\min} = T_0 \Delta S - \Delta H \quad (63.2)$$

where W_{\min} is the minimum work required to produce the process goal, ΔS and ΔH are the difference between product and feed entropy and enthalpy, respectively, and T_0 is the ambient temperature. Table 63.3 lists the minimum work required to liquefy 1 kg-mole of several common cryogenes. Obviously, the lower the temperature level the greater the cost for unit result. The evident conflict in H_2 and He arises from their different molecular weights and properties. However, the temperature differences from ambient to liquid H_2 temperature and from ambient to liquid He temperatures are similar.

A refrigeration cycle that would approach the minimum work calculated as above would include ideal process steps as, for instance, in a Carnot refrigeration cycle. The cryogenic engineer aims for this goal while satisfying practical processing and capital cost limitations.

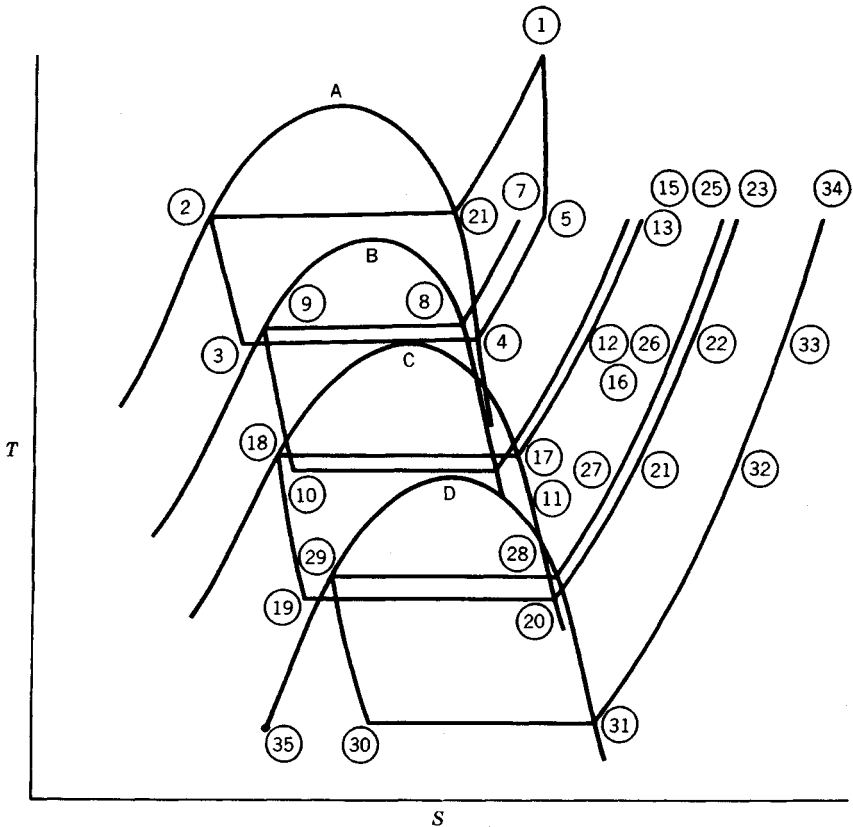
63.2.1 Cascade Refrigeration

The cascade refrigeration cycle was the first means used to liquefy air in the United States.²² It uses conveniently chosen refrigeration cycles, each using the evaporator of the previous fluid cycle as condenser, which will produce the desired temperature. Figures 63.7 and 63.8 show a schematic T - S diagram of such a cycle and the required arrangement of equipment.

Obviously, this cycle is mechanically complex. After its early use it was largely replaced by other cryogenic cycles because of its mechanical unreliability, seal leaks, and poor mechanical efficiency. However, the improved reliability and efficiency of modern compressors has fostered a revival in the cascade cycle. Cascade cycles are used today in some base-load natural gas liquefaction (LNG) plants²³ and in the some peak-shaving LNG plants. They are also used in a variety of intermediate refrigeration processes. The cascade cycle is potentially the most efficient of cryogenic processes

Table 63.3 Minimum Work Required to Liquefy Some Common Cryogenes

Gas	Normal Boiling Point (K)	Minimum Work of Liquefaction (J/mole)
Helium	4.22	26,700
Hydrogen	20.39	23,270
Neon	27.11	26,190
Nitrogen	77.33	20,900
Air	78.8	20,740
Oxygen	90.22	19,700
Methane	111.67	16,840
Ethane	184.50	9,935
Ammonia	239.78	3,961

**Fig. 63.7** Cascade refrigeration system on T - S coordinates. Note that T - S diagram for fluids A, B, C, and D are here superimposed. Numbers here refer to Fig. 63.8 flow points.

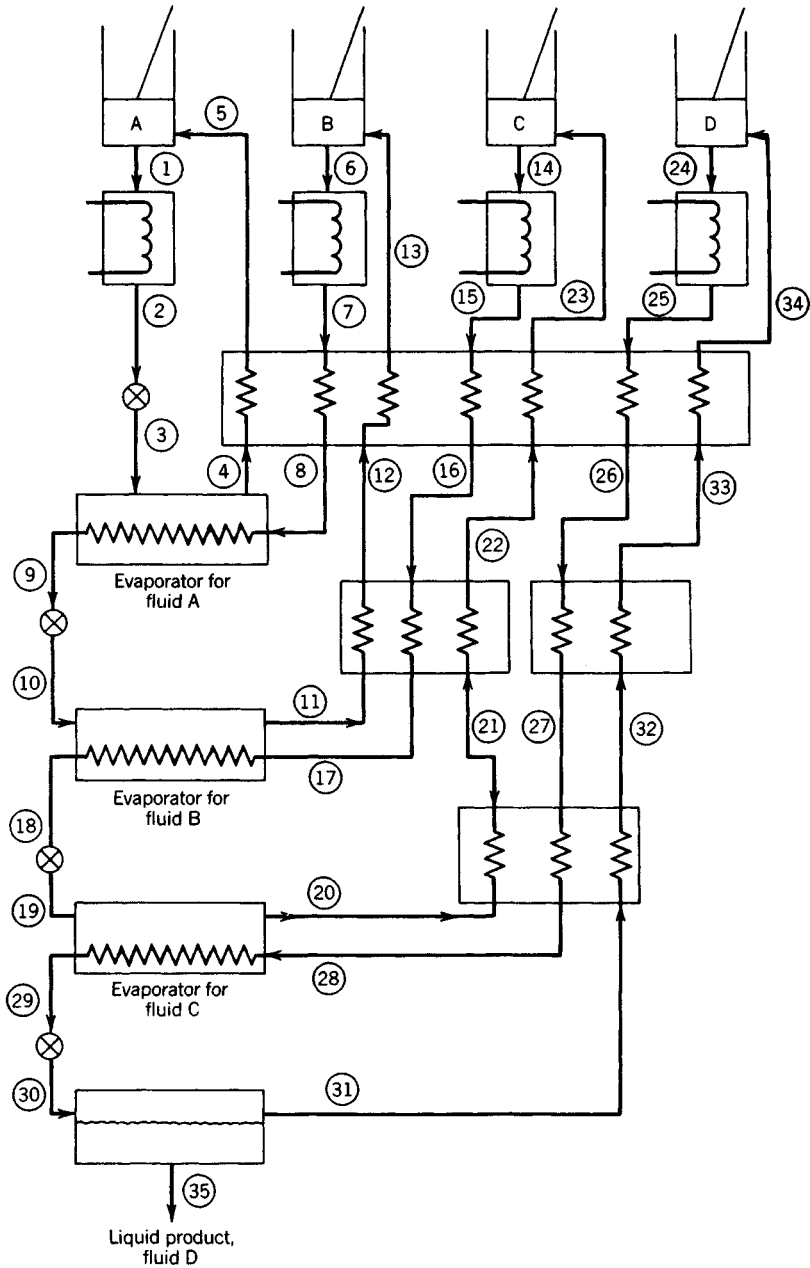


Fig. 63.8 Cascade liquefaction cycle—simplified flow diagram.

because the major heat-transfer steps are liquefaction–vaporization exchanges with each stream at a constant temperature. Thus heat transfer coefficients are high and ΔT s can be kept very small.

63.2.2 The Linde or Joule–Thomson Cycle

The Linde cycle was used in the earliest European efforts at gas liquefaction and is conceptually the simplest of cryogenic cycles. A simple flow sheet is shown in Fig. 63.9. Here the gas to be liquefied

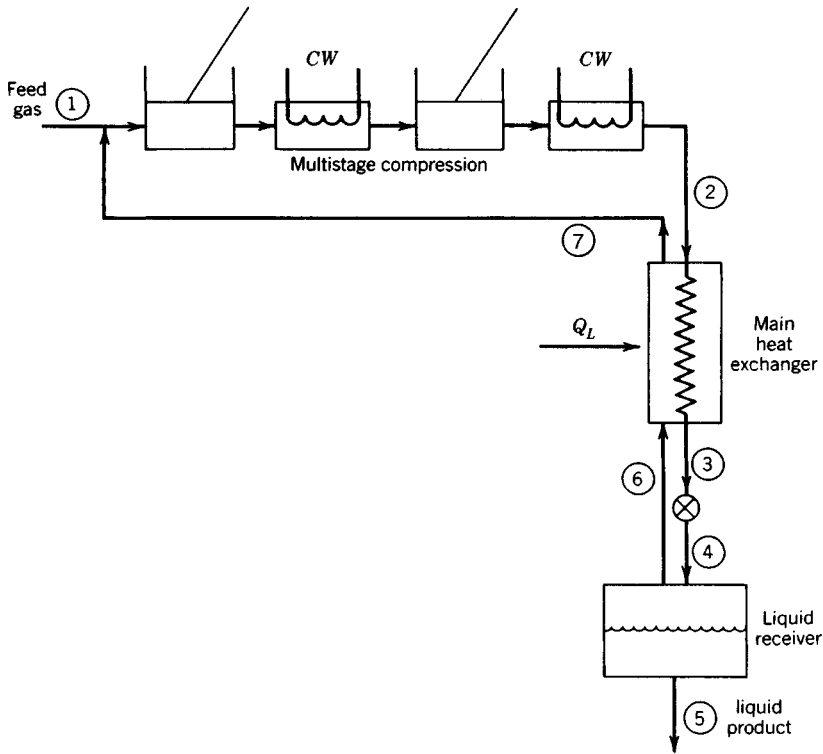


Fig. 63.9 Simplified Joule-Thomson liquefaction cycle flow diagram.

or used as refrigerant is compressed through several stages each with its aftercooler. It then enters the main countercurrent heat exchanger where it is cooled by returning low-pressure gas. The gas is then expanded through a valve where it is cooled by the Joule-Thomson effect and partially liquefied. The liquid fraction can then be withdrawn, as shown, or used as a refrigeration source.

Making a material and energy balance around a control volume including the main exchanger, JT valve, and liquid receiver for the process shown gives

$$X = \frac{(H_7 - H_2) - Q_L}{H_7 - H_5} \quad (63.3)$$

where X is the fraction of the compressed gas to be liquefied. Thus process efficiency and even operability depend entirely on the Joule-Thomson effect at the warm end of the main heat exchanger and on the effectiveness of that heat exchanger. Also, if Q_L becomes large due to inadequate insulation, X quickly goes to zero.

Because of its dependence on Joule-Thomson effect at the warm end of the main exchanger, the Joule-Thomson liquefier is not usable for H_2 and He refrigeration without precooling. However, if H_2 is cooled to liquid N_2 temperature before it enters the JT cycle main heat exchanger, or if He is cooled to liquid H_2 temperature before entering the JT cycle main heat exchanger, further cooling to liquefaction can be done with this cycle. Even with fluids such as N_2 and CH_4 it is often advantageous to precool the gas before it enters the JT heat exchanger in order to take advantage of the greater Joule-Thomson effect at the lower temperature.

63.2.3 The Claude or Expander Cycle

Expander cycles have become workhorses of the cryogenic engineer. A simplified flow sheet is shown in Fig. 63.11. Here part of the compressed gas is removed from the main exchanger before being fully cooled, and is cooled in an expansion engine in which mechanical work is done. Otherwise, the system is the same as the Joule-Thomson cycle. Figure 63.12 shows a T - S diagram for this process. The numbers on the diagram refer to those on the process flow sheet.

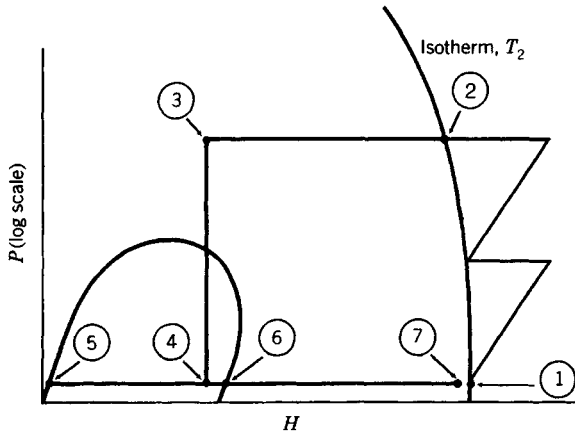


Fig. 63.10 Representation of the Joule-Thomson liquefaction cycle on a P - H diagram.

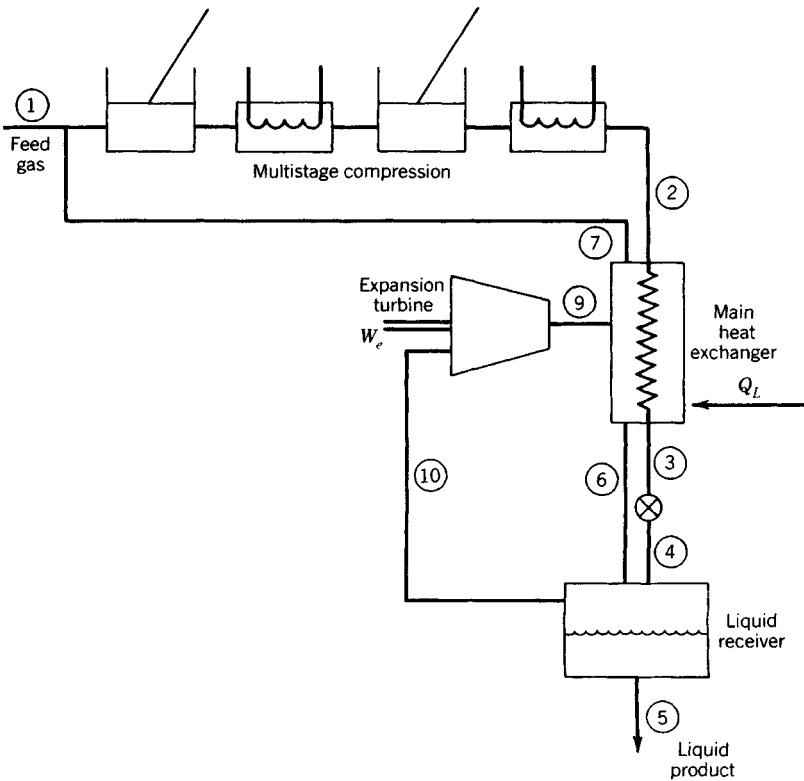


Fig. 63.11 Expander cycle simplified flow diagram.

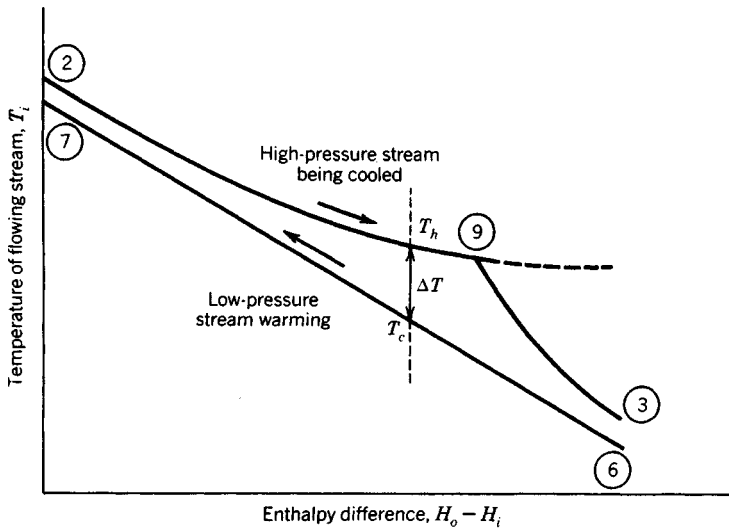


Fig. 63.13 Cooling curves showing temperatures throughout the main exchanger for the expander cycle.

that point is the ΔT available for heat transfer. Obviously, the simple ΔT_{lm} approach to calculation of heat-exchanger area will not be satisfactory here, for that method depends on linear cooling curves. The usual approach here is to divide the exchanger into segments of ΔH such that the cooling curves are linear for the section chosen and to calculate the exchanger area for each section. It is especially important to examine cryogenic heat exchangers in this detail because temperature ranges are likely to be large, thus producing heat-transfer coefficients that vary over the length of the exchanger, and because the curvature of the cooling curves well may produce regions of very small ΔT . In extreme cases the designer may even find that ΔT at some point in the exchanger reaches zero, or becomes negative, thus violating the second law. No exchanger designed in ignorance of this situation would operate as designed.

Minimization of cryogenic process power requirements, and hence operating costs, can be done using classical considerations of entropy gain. For any process

$$W = W_{\min} + \Sigma T_0 \Delta S_T \quad (63.5)$$

where W is the actual work required by the process, W_{\min} is the minimum work [see Eq. (63.1)], and the last term represents the work lost in each process step. In that term T_0 is the ambient temperature, and ΔS_T is the entropy gain of the universe as a result of each process step.

In a heat exchanger

$$T_0 \Delta S_T = W_L = T_0 \int \frac{T_h - T_c}{T_h T_c} dH_i \quad (63.6)$$

where T_h and T_c represent temperatures of the hot and cold streams and the integration is carried out from end to end of the heat exchanger.

A comparison of the Claude cycle (so named because Georges Claude first developed a practical expander cycle for air liquefaction in 1902) with the Joule-Thomson cycle can thus be made by considering the W_L in the comparable process steps. In the cooling curve diagram, Fig. 63.13, the dotted line represents the high-pressure stream cooling curve of a Joule-Thomson cycle operating at the same pressure as does the Claude cycle. In comparison, the Claude cycle produces much smaller ΔT s at the cold end of the heat exchanger. If this is translated into lost work as done in Fig. 63.14, there is considerable reduction. The Claude cycle also reduces lost work by passing only a part of the high-pressure gas through a valve, which is a completely irreversible pressure reduction step. The rest of the high-pressure gas is expanded in a machine where most of the pressure lost produces usable work.

There are other ways to reduce the ΔT , and hence the W_L , in cryogenic heat exchangers. These methods can be used by the engineer as process conditions warrant. Figure 63.15 shows the effect

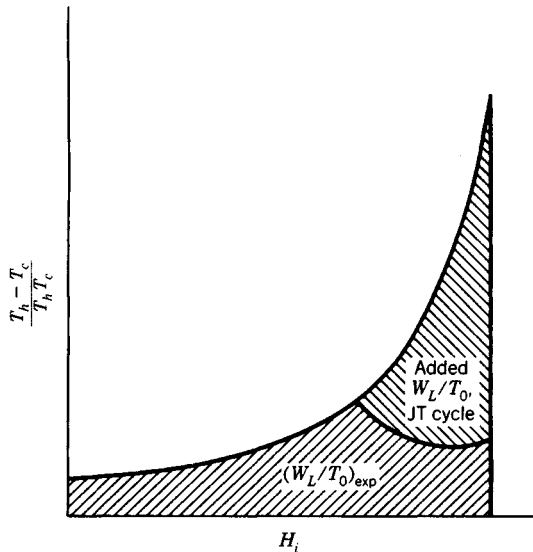


Fig. 63.14 Calculation of W_L in the main heat exchanger using Eq. (63.6) and showing the comparison between JT and Claude cycles.

of (a) intermediate refrigeration, (b) varying the amount of low-pressure gas in the exchanger, and (c) adding a third cold stream to the exchanger.

63.2.4 Low-Temperature Engine Cycles

The possibility that Carnot cycle efficiency could be approached by a refrigeration cycle in which all pressure change occurs by compression and expansion has encouraged the development of several cycles that essentially occur within an engine. In general, these have proven useful for small-scale cryogenic refrigeration under unusual conditions as in space vehicles. However, the Stirling cycle, discussed below, has been used for industrial-scale production situations.

The Stirling Cycle

In this cycle a noncondensable gas, usually helium, is compressed, cooled both by heat transfer to cooling water and by heat transfer to a cold solid matrix in a regenerator (see Section 63.3.3), and expanded to produce minimum temperature. The cold gas is warmed by heat transfer to the fluid or space being refrigerated and to the now-warm matrix in the regenerator and returned to the compressor. Figure 63.16 shows the process path on a T - S diagram. The process efficiency of this idealized cycle is identical to a Carnot cycle efficiency.

In application the Stirling cycle is usually operated in an engine where compression and expansion both occur rapidly with compression being nearly adiabatic. Figure 63.17 shows such a machine. The compressor piston (1) and a displacer piston (16 with cap 17) operate off the same crankshaft. Their motion is displaced by 90° . The result is that the compressor position is near the top or bottom of its cycle as the displacer is in most rapid vertical movement. Thus the cycle can be traced as follows:

1. With the displacer near the top of its stroke the compressor moves up compressing the gas in space 4.
2. The displacer moves down, and the gas moves through the annular water-cooled heat exchanger (13) and the annular regenerator (14) reaching the upper space (5) in a cooled, compressed state. The regenerator packing, fine copper wool, is warmed by this flow.
3. Displacer and compressor pistons move down together. Thus the gas in (5) is expanded and cooled further. This cold gas receives heat from the chamber walls (18) and interior fins (15) thus refrigerating these solid parts and their external finning.
4. The displacer moves up, thus moving the gas from space (5) to space (4). In flowing through the annular passages the gas recools the regenerator packing.

The device shown in Fig. 63.17 is arranged for air liquefaction. Room air enters at (23), passes through the finned structure where water and then CO_2 freeze out, and is then liquified as it is further

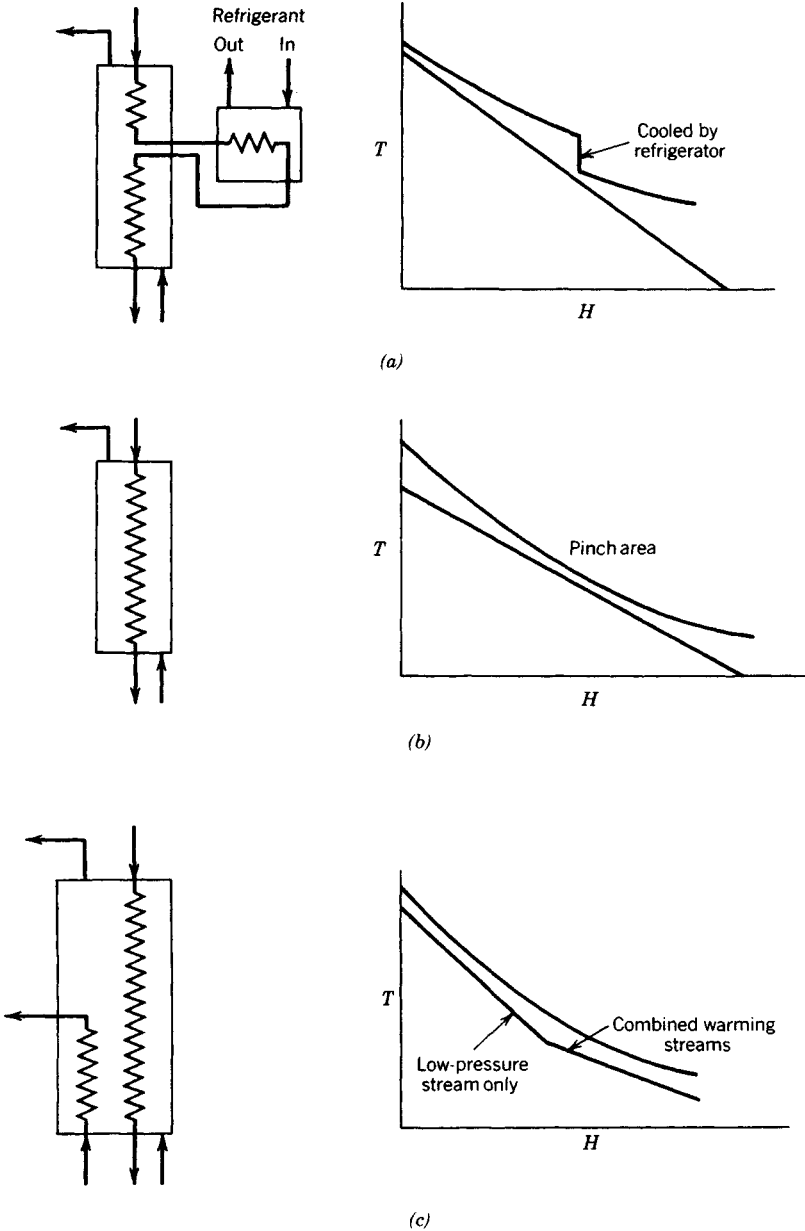


Fig. 63.15 Various cooling curve configurations to reduce W_L : (a) Cooling curve for intermediate refrigerator case. (b) Use of reduced warming stream to control ΔT s. (c) Use of an additional warming stream.

cooled as it flows over the finned surface (18) of the cylinder. The working fluid, usually He, is supplied as needed from the tank (27).

Other Engine Cycles

The Stirling cycle can be operated as a heat engine instead of as a refrigerator and, in fact, that was the original intent. In 1918 Vuilleumier patented a device that combines these two forms of Stirling cycle to produce a refrigerator that operated on a high-temperature heat source rather than on a source

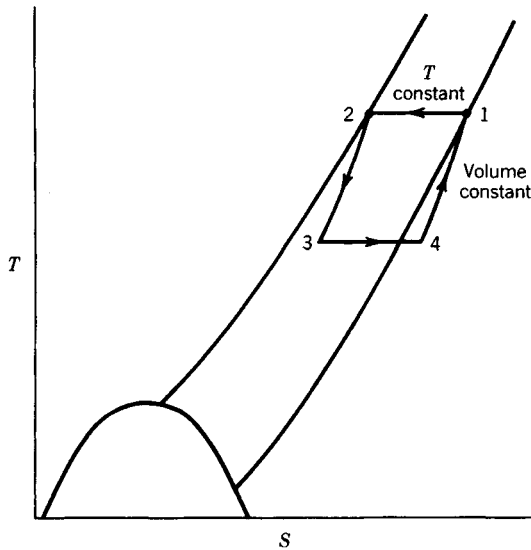


Fig. 63.16 The idealized Stirling cycle represented on a T - S diagram.

of work. This process has received recent attention²⁴ and is useful in situations where a heat source is readily available but where power is inaccessible or costly.

The Gifford-McMahon cycles²⁵ have proven useful for operations requiring a light-weight, compact refrigeration source. Two cycles exist: one with a displacer piston that produces little or no work; the other with a work-producing expander piston. Fig 63.18 shows the two cycles.

In both these cycles the compressor operates continuously maintaining the high-pressure surge volume of P_1 , T_1 . The sequence of steps for the system with work-producing piston are:

1. Inlet valve opens filling system to P_2 .
2. Gas enters the cold space below the piston as the piston moves up doing work and thus cooling the gas. The piston continues, reducing the gas pressure to P_1 .
3. The piston moves down pushing the gas through the heat load area and the regenerator to the storage vessel at P_1 .

The sequence of steps for the system with the displacer is similar except that gas initially enters the warm end of the cylinder, is cooled by the heat exchanger, and then is displaced by the piston so that it moves through the regenerator for further cooling before entering the cold space. Final cooling is done by "blowing down" this gas so that it enters the low-pressure surge volume at P_1 .

If the working fluid is assumed to be an ideal gas, all process steps are ideal, and compression is isothermal, the COPs for the two cycles are:

$$\text{COP (work producing)} = 1 \left/ \frac{RT_1 \ln P_2/P_1}{C_{P_0} T_3 [1 - (P_4/P_3)^{(k-1)/k}]^{-1}} \right.$$

$$\text{COP (displacer)} = \frac{P_3 - P_1}{P_3(T_1/T_3 - P_1/P_3) \ln P_2/P_1}$$

In these equations states 1 and 2 are those immediately before and after the compressor. State 3 is after the cooling step but before expansion, and state 4 is after the expansion at the lowest temperature.

63.3 CRYOGENIC HEAT-TRANSFER METHODS

In dealing with heat-transfer requirements the cryogenic engineer must effect large quantities of heat transfer over small ΔT s through wide temperature ranges. Commonly heat capacities and/or mass flows change along the length of the heat-transfer path, and often condensation or evaporation takes place. To minimize heat leak these complexities must be handled using exchangers with as large a heat-transfer surface area per exchanger volume as possible. Compact heat-exchanger designs of many sorts have been used, but only the most common types will be discussed here.

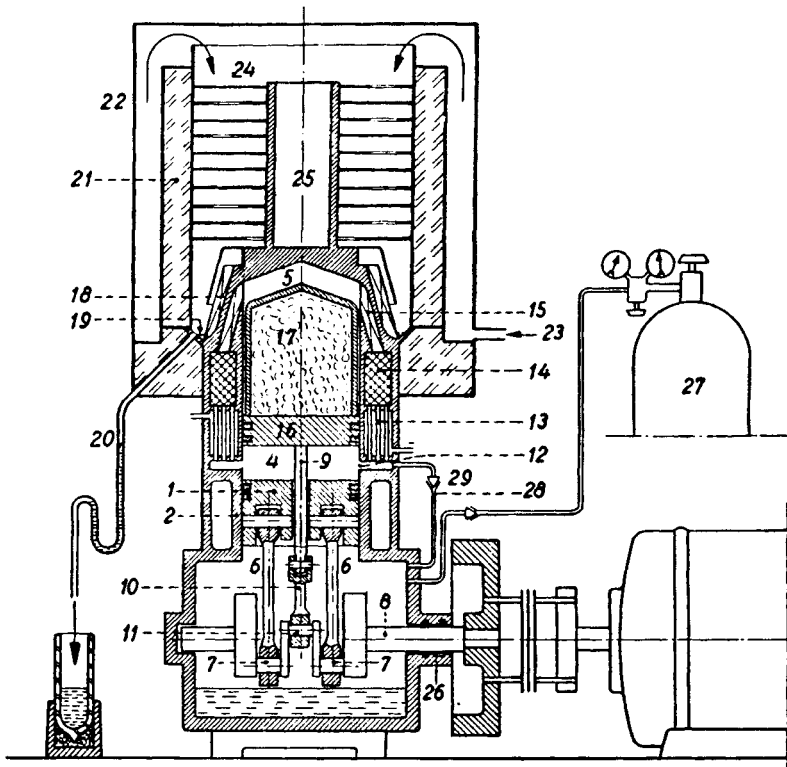


Fig. 63.17 Stirling cycle arranged for air liquefaction reference points have the following meanings: 1, compressor; 2, compression cylinder; 4, working fluid in space between compressor and displacer; 5, working fluid in the cold head region of the machine; 6, two parallel connecting rods with cranks; 7, of the main piston; 8, crankshaft; 9, displacer rod, linked to connecting rod, 10, and crank, 11, of the displacer; 12, ports; 13, cooler; 14, regenerator; 15, freezer; 16, displacer piston, and 17, cap; 18, condenser for the air to be liquefied, with annular channel, 19, tapping pipe (gooseneck) 20, insulating screening cover, 21, and mantel 22; 23, aperture for entry of air; 24, plates of the ice separator, joined by the tubular structure, 25, to the freezer (15); 26, gas-tight shaft seal; 27, gas cylinder supplying refrigerant; 28, supply pipe with one-way valve, 29. (Courtesy U.S. Philips Corp.)

63.3.1 Coiled-Tube-in-Shell Exchangers

The traditional heat exchanger for cryogenic service is the Hampson or coiled-tube-in-shell exchanger as shown in Fig. 63.19. The exchanger is built by turning a mandrel on a specially built lathe, and wrapping it with successive layers of tubing and spacer wires. Since longitudinal heat transfer down the mandrel is not desired, the mandrel is usually made of a poorly conducting material such as stainless steel, and its interior is packed with an insulating material to prevent gas circulation. Copper or aluminum tubing is generally used. To prevent uneven flow distribution from tube to tube, tube winding is planned so that the total length of each tube is constant independent of the layer on which the tube is wound. This results in a constant winding angle, as shown in Fig. 63.20. For example, the tube layer next to the mandrel might have five parallel tubes, whereas the layer next to the shell might have 20 parallel tubes. Spacer wires may be laid longitudinally on each layer of tubes, or they may be wound counter to the tube winding direction, or omitted. Their presence and size depends on the flow requirements for fluid in the exchanger shell. Successive tube layers may be wound in opposite or in the same direction.

After the tubes are wound on the mandrel they are fed into manifolds at each end of the tube bundle. The mandrel itself may be used for this purpose, or hook-shaped manifolds of large diameter tubing can be looped around the mandrel and connected to each tube in the bundle. Finally, the exchanger is closed by wrapping a shell, usually thin-walled stainless steel, over the bundle and welding on the required heads and nozzles.

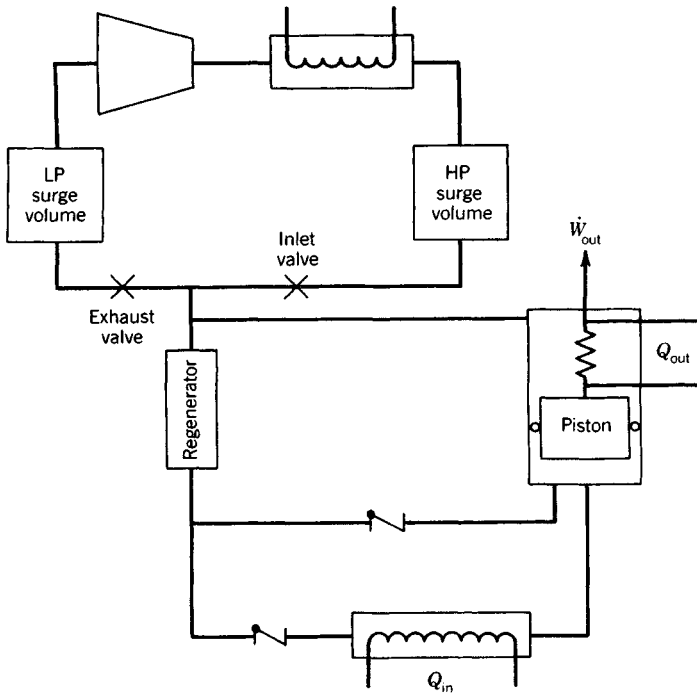


Fig. 63.18 Gifford-McMahon refrigerator. The dashed line and the cooler are present only when the piston is to be used as a displacer with negligible work production.

In application the low-pressure fluid flows through the exchanger shell, and high-pressure fluids flow through the tubes. This exchanger is easily adapted for use by three or more fluids by putting in a pair of manifolds for each tube-side fluid to be carried. However, tube arrangement must be carefully engineered so that the temperatures of all the cooling streams (or all the warming streams) will be identical at any given exchanger cross section. The exchanger is typically mounted vertically so that condensation and gravity effects will not result in uneven flow distribution. Most often the cold end is located at the top so that any liquids not carried by the process stream will move toward warmer temperatures and be evaporated.

Heat-transfer coefficients in these exchangers will usually vary from end to end of the exchangers because of the wide temperature range experienced. For this reason, and because of the nonlinear ΔT

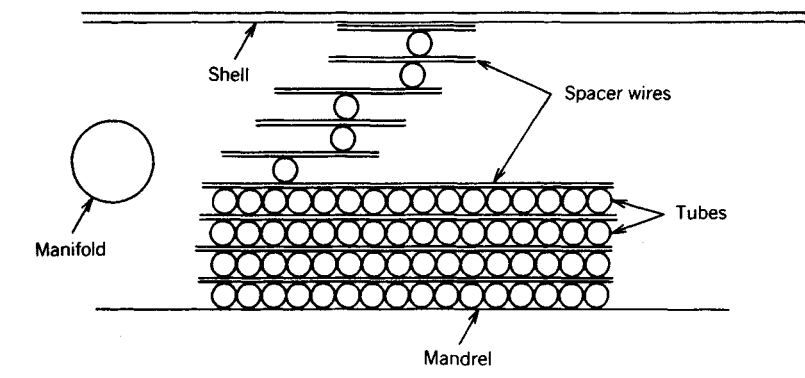


Fig. 63.19 Section of a coiled-tube-in-shell heat exchanger.

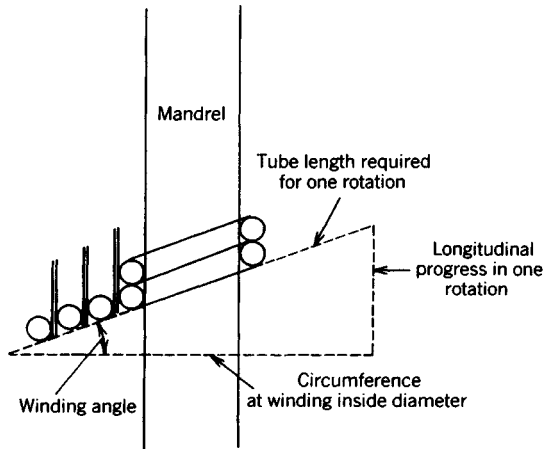


Fig. 63.20 Winding relationships for a coiled-tube-in-shell exchanger.

variations, the exchanger area must be determined by sections, the section lengths chosen so that linear ΔT s can be used and so that temperature ranges are not excessive. For inside tube heat-transfer coefficients with single-phase flow the Dittus–Boelter equation is used altered to account for the spiral flow:

$$\frac{hD}{k} = 0.023 N_{Re}^{0.8} N_{Pn}^{0.32} \left(1 + 3.5 \frac{d}{D} \right) \quad (63.7)$$

where D is the diameter of the helix and d the inside diameter.

For outside heat-transfer coefficients the standard design methods for heat transfer for flow across tube banks with in-line tubes are used. Usually the metal wall resistance is negligible. In some cases adjacent tubes are brazed or soldered together to promote heat transfer from one to the other. Even here wall resistance is usually a very small part of the total heat-transfer resistance.

Pressure drop calculations are made using equivalent design tools. Usually the low-pressure-side ΔP is critical in designing a usable exchanger.

The coiled-tube-in-shell exchanger is expensive, requiring a large amount of hand labor. Its advantages are that it can be operated at any pressure the tube can withstand, and that it can be built over very wide size ranges and with great flexibility of design. Currently these exchangers are little used in standard industrial cryogenic applications. However, in very large sizes (14 ft diameter \times 120 ft length) they are used in base-load natural gas liquefaction plants, and in very small size (finger sized) they are used in cooling sensors for space and military applications.

63.3.2 Plate-Fin Heat Exchangers

The plate-fin exchanger has become the most common type used for cryogenic service. This results from its relatively low cost and high concentration of surface area per cubic foot of exchanger volume. It is made by clamping together a stack of alternate flat plates and corrugated sheets of aluminum coated with brazing flux. This assembly is then immersed in molten salt where the aluminum brazes together at points of contact. After removal from the bath the salt and flux are washed from the exchanger paths, and the assembly is enclosed in end plates and nozzles designed to give the desired flow arrangement. Usually the exchanger is roughly cubic, and is limited in size by the size of the available salt bath and the ability to make good braze seals in the center of the core. The core can be arranged for countercurrent flow or for cross flow. Figure 63.21 shows the construction of a typical plate-fin exchanger.

Procedures for calculating heat-transfer and pressure loss characteristics for plate-fin exchangers have been developed and published by the exchanger manufacturers. Table 63.4 and Fig. 63.22 present one set of these.

63.3.3 Regenerators

A regenerator is essentially a storage vessel filled with particulate solids through which hot and cold fluid flow alternately in opposite directions. The solids absorb energy as the hot fluid flows through, and then transfer this energy to the cold fluid. Thus this solid acts as a short-term energy-storage

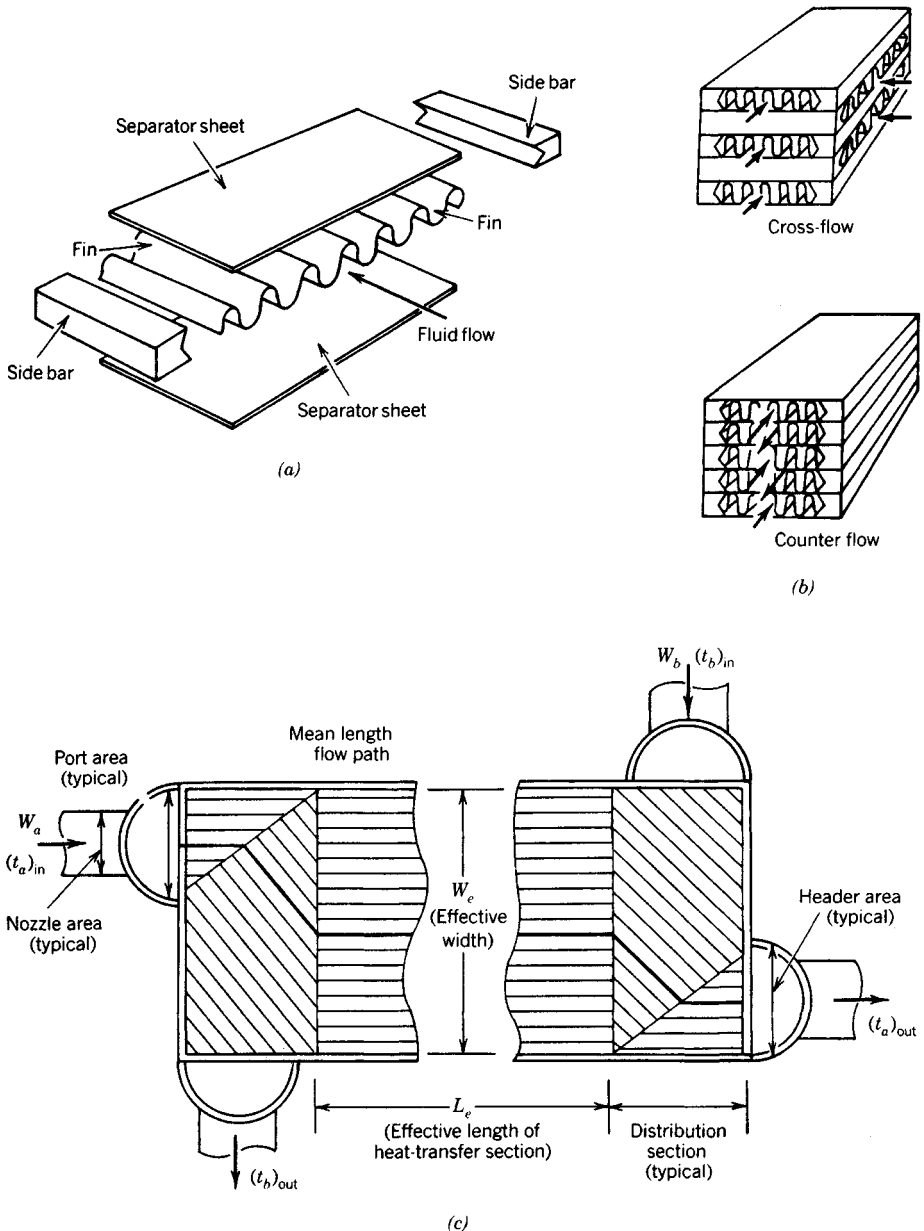


Fig. 63.21 Construction features of a plate-fin heat exchanger. (a) Detail of plate and fin. (b) Flow arrangements. (c) Total assembly arrangement.

medium. It should have high heat capacity and a large surface area, but should be designed as to avoid excessive flow pressure drop.

In cryogenic service regenerators have been used in two very different applications. In engine liquefiers very small regenerators packed with, for example, fine copper wire have been used. In these situations the alternating flow direction has been produced by the intake and exhaust strokes of the engine. In air separation plants very large regenerators in the form of tanks filled with pebbles have been used. In this application the regenerators have been used in pairs with one regenerator

Table 63.4 Computation of Fin Surface Geometrics^a

Fin Height (in.)	Type of Surface	Fin Spacing (FPI)	Fin Thickness (in.)	A'_c	A'_{ht}	B	r_h	A_r/A_{ht}
0.200	Plain or perforated	14	0.008	0.001185	0.596	437	0.001986	0.751
0.200	Plain or perforated	14	0.012	0.001086	0.577	415	0.001884	0.760
0.250	Plain or perforated	10	0.025	0.001172	0.500	288	0.00234	0.750
0.375	Plain or perforated	8	0.025	0.001944	0.600	230	0.003240	0.778
0.375	Plain or perforated	15	0.008	0.00224	1.064	409	0.00211	0.862
0.250	1/8 lanced	15	0.012	0.001355	0.732	420	0.001855	0.813
0.250	1/8 lanced	14	0.020	0.001150	0.655	378	0.001751	0.817
0.375	1/8 lanced	15	0.008	0.00224	1.064	409	0.002108	0.862
0.455	Ruffled	16	0.005	0.002811	1.437	465	0.001956	0.893

^a Definition and use of terms:

FPI = fins per inch

A'_c = free stream area factor, ft²/passage/in. of effective passage width

A'_{ht} = heat-transfer area factor, ft²/passage/in./ft of effective length

B = heat-transfer area per unit volume between plates, ft²/ft³

r_h = hydraulic radius = cross section area/wetted perimeter, ft

A_r = effective heat-transfer area = $A_{ht} \cdot \eta_0$

A_{ht} = total heat-transfer area

η_0 = weighted surface effectiveness factor

= $1 - (A_r/A_{ht})(1 - \eta_f)$

A_f = fin heat-transfer area

η_f = fin efficiency factor = $[\tanh(ml)]/ml$

ml = fin geometry and material factor = $(b/s) \sqrt{2h/k}$

b = fin height, ft

h = film coefficient for heat transfer, Btu/hr · ft² · °F

k = thermal conductivity of the fin material, Btu/hr · ft · °F

s = fin thickness, ft

U = overall heat transfer coefficient = $1/(A/h_a A_a + A/h_b A_b)$

a, b = subscripts indicating the two fluids between which heat is being transferred

Courtesy Stewart-Warner Corp.

receiving hot fluid as cold fluid enters the other. Switch valves and check valves are used to alternate flow to the regenerator bodies, as shown in Fig. 63.23.

The regenerator operates in cyclical, unsteady-state conditions. Partial differential equations can be written to express temperatures of gas and of solid phase as a function of time and bed position under given conditions of flow rates, properties of gaseous and solid phases, and switch time. Usually these equations are solved assuming constant heat capacities, thermal conductivities, heat-transfer coefficients, and flow rates. It is generally assumed that flow is uniform throughout the bed cross section, that the bed has infinite conductivity in the radial direction but zero in the longitudinal direction, and that there is no condensation or vaporization occurring. Thermal gradients through the solid particles are usually ignored. These equations can then be solved by computer approximation. The results are often expressed graphically.²⁶

An alternative approach compares the regenerator with a steady-state heat exchanger and uses exchanger design methods for calculating regenerator size.²⁷ Figure 63.24 shows the temperature-time relationship at several points in a regenerator body. In the central part of the regenerator ΔT s are nearly constant throughout the cycle. Folding the figure at the switch points superimposes the temperature data for this central section as shown in Fig. 63.25. It is clear that the solid plays only a time-delaying function as energy flows from the hot stream to the cold one. Temperature levels are set by the thermodynamics of the cooling curve such as Fig. 63.15 presents. Thus the $q = UA\Delta T$ equation can be used for small sections of the regenerator if a proper U can be determined.

During any half cycle the resistance to heat transfer from the gas to the solid packing will be just the gas-phase film coefficient. It can be calculated from empirical correlations for the packing material in use. For pebbles, the correlations for heat transfer to spheres in a packed bed²⁸ is normally used to obtain the film coefficient for heat transfer from gas to solid:

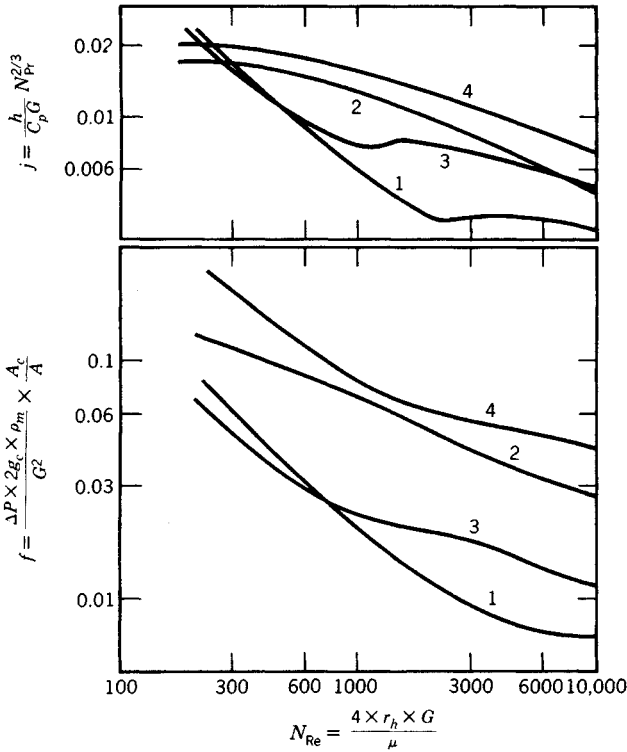


Fig. 63.22 Heat-transfer and flow friction factors in plate and fin heat exchangers. Curves 1: plain fin (0.200 in. height, 14 fins/in.—0.008 in. thick). Curves 2: ruffled fin (0.445 in. height, 16 fins/in.—0.005 in. thick). Curves 3: perforated fin (0.375 in. height, 8 fins/in.—0.025 in. thick). (Courtesy Stewart-Warner Corp.)

$$h_{gs} = 1.31(G/d)^{0.93} \tag{63.8}$$

where h_{gs} = heat transfer from gas to regenerator packing or reverse, J/hr · m² · K
 G = mass flow of gas, kg/hr · m²
 d = particle diameter, m

The heat that flows to the packing surface diffuses into the packing by a conductive mode. Usually this transfer is fast relative to the transfer from the gas phase, but it may be necessary to calculate solid surface temperatures as a function of heat-transfer rate and adjust the overall ΔT accordingly. The heat-transfer mechanisms are typically symmetrical and hence the design equation becomes

$$A = \frac{q}{U\Delta T} = \frac{q}{h/2 \times \Delta T/2} = \frac{4q}{h_{gs}\Delta T}$$

This calculation can be done for each section of the cooling curve until the entire regenerator area is calculated. However, at the ends of the regenerator temperatures are not symmetrical nor is the ΔT constant throughout the cycle. Figure 63.26 gives a correction factor that must be used to adjust the calculated area for these end effects. Usually a 10–20% increase in area results.

The cyclical nature of regenerator operation allows their use as trapping media for contaminants simultaneously with their heat-transfer function. If the contaminant is condensable, it will condense and solidify on the solid surfaces as the cooling phase flows through the regenerator. During the warming phase flow, this deposited condensed phase will evaporate flowing out with the return media.

Consider an air-separation process in which crude air at a moderate pressure is cooled by flow through a regenerator pair. The warmed regenerator is then used to warm up the returning nitrogen

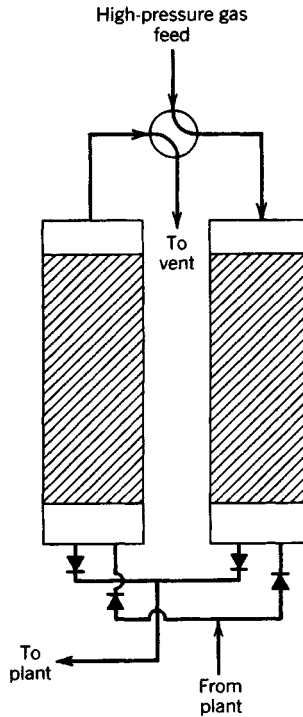


Fig. 63.23 Regenerator pair configuration.

at low pressure. The water and CO_2 in the air deposit on the regenerator surfaces and then reevaporate into the nitrogen. If deposition occurs at thermodynamic equilibrium, and assuming Raoult's law,

$$y_{\text{H}_2\text{O}} \text{ or } y_{\text{CO}_2} = \frac{P^\circ_{\text{H}_2\text{O or CO}_2}}{P} \quad (63.9)$$

where y = mole fraction of H_2O or CO_2 in the gas phase

P° = saturation vapor pressure of H_2O or CO_2

P = total pressure of flowing stream

This equation can be applied to both the depositing, incoming situation and the reevaporating, outgoing situation. If the contaminant is completely removed in the regenerator, and the return gas is pure as it enters the regenerator, the moles of incoming gas times the mole fraction of contaminant must equal that same product for the outgoing stream if the contaminant does not accumulate in the regenerator. Since the vapor pressure is a function of temperature, and the returning stream pressure is lower than the incoming stream pressure, these relations can be combined to give the maximum stream-to-stream ΔT that may exist at any location in the regenerator. Figure 63.27 shows the results for one regenerator design condition. Also plotted on Fig. 63.27 is a cooling curve for these same design conditions. At the conditions given H_2O will be removed down to very low concentrations, but CO_2 solids may accumulate in the bottom of the regenerator. To prevent this it would be necessary to remove some of the air stream in the middle of the regenerator for further purification and cooling elsewhere.

Cryogenic heat exchangers often are called on to condense or evaporate and two-phase heat-transfer commonly occurs, sometimes on both sides of a given heat exchanger. Heat-transfer coefficients and flow pressure losses are calculated using correlations taken from high-temperature data.²⁹ The distribution of multiphase processing streams into parallel channels is, however, a common and severe problem in cryogenic processing. In heat exchangers thousands of parallel paths may exist. Thus the designer must ensure that all possible paths offer the same flow resistance and that the two

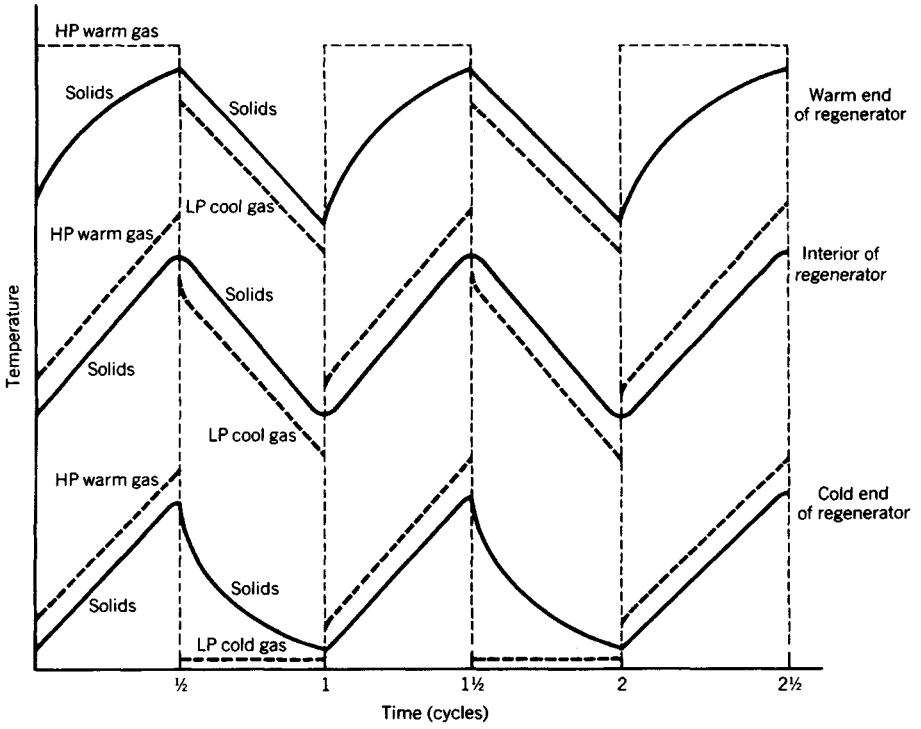


Fig. 63.24 Time-temperature histories in a regenerator.

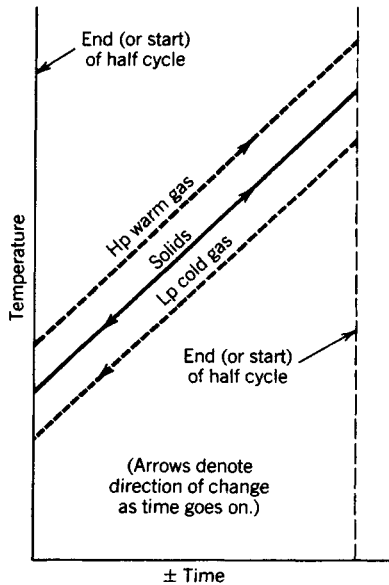


Fig. 63.25 Time-temperature history for a central slice through a regenerator.

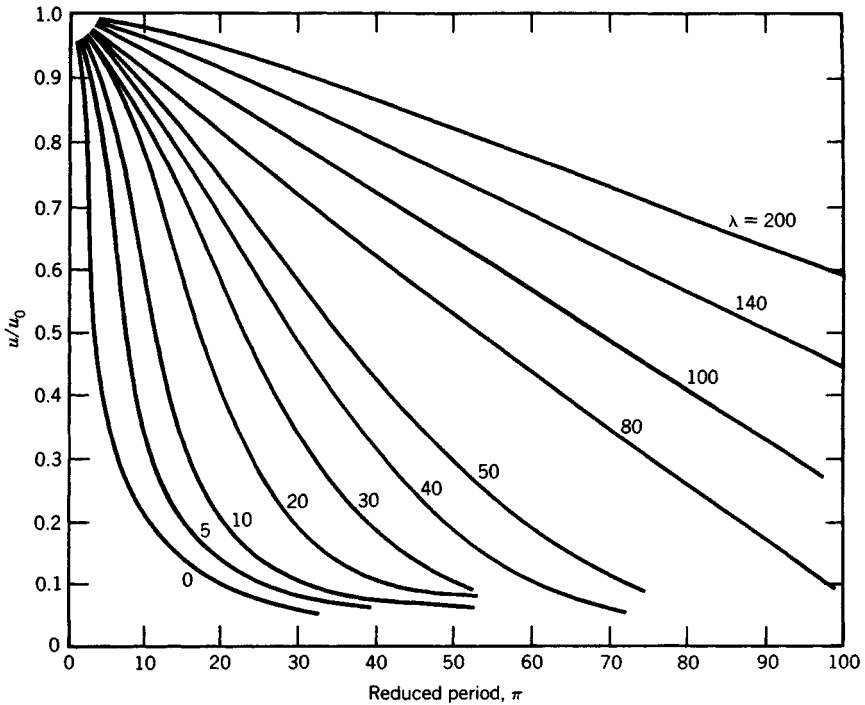


Fig. 63.26 End correction for regenerator heat transfer calculation using symmetrical cycle theory²⁷ (courtesy Plenum Press):

$$\lambda = \frac{4H_0S(T_c + T_w)}{C_cT_c + C_wT_w} = \text{reduced length}$$

$$\pi = \frac{12H_0(T_c + T_w)}{c\rho_s d} = \text{reduced period}$$

$$U_0 = \frac{1}{4} \left[\frac{1}{h} + \frac{0.1d}{k} \right]$$

where T_w, T_c = switching times of warm and cold streams, respectively, hr

S = regenerator surface area, m^2

U_0 = overall heat transfer coefficient uncorrected for hysteresis, $kcal/m^2 \cdot hr \cdot ^\circ C$

U = overall heat transfer coefficient

C_w, C_c = heat capacity of warm and cold stream, respectively, $kcal/hr \cdot ^\circ C$

c = specific heat of packing, $kcal/kg \cdot ^\circ C$

d = particle diameter, m

ρ_s = density of solid, kg/m^3

phases are well distributed in the flow stream approaching the distribution point. Streams that cool during passage through an exchanger are likely to be modestly self-compensating in that the viscosity of a cold gas is lower than that of a warmer gas. Thus a stream that is relatively high in temperature (as would be the case if that passage received more than its share of fluid) will have a greater flow resistance than a cooler system, so flow will be reduced. The opposite effect occurs for streams being warmed, so that these streams must be carefully balanced at the exchanger entrance.

63.4 INSULATION SYSTEMS

Successful cryogenic processing requires high-efficiency insulation. Sometimes this is a processing necessity, as in the Joule-Thomson liquefier, and sometimes it is primarily an economic requirement, as in the storage and transportation of cryogenes. For large-scale cryogenic processes, especially those operating at liquid nitrogen temperatures and above, thick blankets of fiber or powder insulation, air